

Electrodes from carbonized grass clippings for bioelectrochemical systems

Alexander Langsdorf^a, Michael Halim^a, Marianne Volkmar^b, Markus Stöckl^c, Ralf Harnisch^d, Peter Hahn^d, Roland Ulber^b, Dirk Holtmann^{a,e,*}

^a Institute of Bioprocess Engineering and Pharmaceutical Technology, University of Applied Sciences Mittelhessen, Wiesenstrasse 14, 35390 Giessen, Germany

^b Institute of Bioprocess Engineering, University of Kaiserslautern-Landau, Gottlieb-Daimler-Straße 49, 67663 Kaiserslautern, Germany

^c Chemical Technology, DECHEMA Research Institute, Theodor-Heuss-Allee 25, 60486 Frankfurt am Main, Germany

^d ifn Forschungs- und Technologiezentrum GmbH, Dr.-Bergius-Straße 19, 06729 Elsteraue, Germany

^e Institute of Process Engineering in Life Sciences, Karlsruhe Institute of Technology, Fritz-Haber-Weg 4, 76131 Karlsruhe, Germany

ARTICLE INFO

Keywords:

Green waste
Biochar
Electrode
Microbial electrosynthesis
Microbial fuel cell
Biorefinery

ABSTRACT

One major obstacle to the commercialization of electrobiotechnological systems is the cost of materials, including expensive electrodes. Smart recycling as well as the use of renewable resources can contribute to producing electrodes more ecologically and economically. Green waste is a biogenic residual material that occurs mainly in urban areas and is currently not recycled to a sufficient extent. Here we show the fabrication of electrodes from carbonized grass clippings and their application in microbial electrosynthesis as well as microbial fuel cells. While the electrodes cannot compete with established metal competitors for water electrolysis in microbial electrosynthesis, they perform comparably to commercial graphite electrodes in microbial fuel cells. With *Geobacter sulfurreducens*, a current response can be recorded for more than six weeks. To the best of our knowledge, this is the first time that carbonized green waste has been used as an electrode material for bioelectrochemical systems. This demonstrates the potential of carbonized biological materials as a raw material for electrodes and presents a recycling alternative for green waste.

1. Introduction

Electrobiotechnology is an emerging field that offers new opportunities in industry by combining electrochemical and biotechnological processes. By combining biotechnology with electrochemistry, bioprocesses can be intensified (Stöckl et al., 2023). Thanks to the new opportunities that are emerging, electrobiotechnology can substantially contribute to the realization of the UN Sustainable Development Goals (Gizewski et al., 2023). Bioelectrochemical systems use electroactive microorganisms capable of generating electric current or accepting electrons, for example, to convert CO₂ (Logan et al., 2019). Two of the most promising technologies are the microbial fuel cell and microbial electrosynthesis.

In the process of microbial electrosynthesis (MES), microorganisms can accept electrons from electrodes via different electron transfer mechanisms and use them as an energy source to produce basic chemicals. This allows the energy industry and the chemical or biotechnological industry to be linked. From various options for the MES, the use of secondary microbial electrochemical technology, meaning the

integration of microbial conversions into electrosynthesis, is the most technically advanced, along with hybrid systems (Fruehauf et al., 2020). Indirect electron transport from electrodes to microorganisms can take place via hydrogen generated by water electrolysis. *Cupriavidus necator* is one such organism that is able to grow autotrophically by utilizing H₂ as electron donor, O₂ as electron acceptor, and CO₂ as carbon source. For example, we have shown that we could produce the sesquiterpene α -humulene via microbial electrosynthesis using a genetically modified *C. necator* strain (Krieg et al., 2018) or use Kolbe electrolysis waste gases for the synthesis of fuels and solvents (Teetz et al., 2022). By using exhaust gas CO₂ and renewable electrical energy, a green process can be created. However, for MES to be economically efficient, investment and operational costs must be reduced.

Microbial fuel cells (MFC) can be used in wastewater treatment plants to generate electricity using electroactive microorganisms to transfer electrons to electrodes by converting organic substances. In such real applications, mixed microbial cultures are usually present. In mixed cultures from different sources, *Geobacter sulfurreducens* is substantially responsible for the performance of the MFC (G. Sun et al.,

* Corresponding author.

E-mail address: dirk.holtmann@kit.edu (D. Holtmann).

<https://doi.org/10.1016/j.clce.2024.100118>

Received 5 March 2024; Received in revised form 30 April 2024; Accepted 9 May 2024

Available online 10 May 2024

2772-7823/© 2024 The Authors. Published by Elsevier Ltd. This is an open access article under the CC BY license (<http://creativecommons.org/licenses/by/4.0/>).

2016). Therefore, the model organism *G. sulfurreducens* is often used in the MFC in laboratory experiments. It was shown that *G. sulfurreducens* is able to use graphite electrodes as the electron acceptor, allowing the production of electrical current through the oxidation of acetate (Bond and Lovley, 2003; Stöckl et al., 2019). The organism uses pili to form a biofilm on the electrode (Reguera et al., 2007). These also serve as electrical nanowires for direct electron transfer from the cell to the electrode surface (Reguera et al., 2005). As a result, the anode has a decisive influence on the performance of the MFC. The technical requirements for the individual components of a bioelectrochemical system including the electrodes are described in detail in the review article by Krieg et al. (Krieg et al., 2014). As described, there are different electron transfer mechanisms depending on the technology. Accordingly, the requirements for the electrodes vary depending on the bioelectrochemical system and the microorganisms used (e.g. biofilm formers or indirect electron transfer).

Carbon materials such as graphite have long been used as electrodes. The mining and production of graphite is an energy-intensive, time-consuming, and therefore expensive process (Jara et al., 2019). While graphite electrodes are traditionally made from fossil resources, biomass can serve as an alternative raw material for graphite electrode production. Biomass can be carbonized to obtain a biochar with a high graphite content (Zhang et al., 2021). The use of electrodes made from renewable raw materials can help to reduce investment and operating costs and can also have ecological advantages (Yang and Chen, 2020).

Many publications can be found on the hydrothermal carbonization of lignocellulosic waste biomass for different applications. However, the relatively low temperatures lead to a low degree of graphitization resulting in biochar with poor conductivity (Yang and Chen, 2020). Instead, additional pyrolysis of the biomass at higher temperatures is required. The production of biochar by pyrolysis has already been demonstrated from a variety of different lignocellulosic biomasses such as palm leaves (Ferreira et al., 2018), brewers' spent grain (Cancelliere et al., 2019), peanut shells (Zhan et al., 2021), *Cotinus coggygia* flowers (Li et al., 2020), maple wood (Zhang et al., 2014), vineyard residues (V. Hoffmann et al., 2019), or corncob (V. Hoffmann et al., 2019). In many cases, biochars have been investigated as an electrode material for supercapacitors e.g. from pyrolyzed peanut shells (Purkait et al., 2017), pyrolyzed fungi (Zhu et al., 2011), or pyrolyzed corn straw (Qiu et al., 2018). However, the application in bioelectrochemical systems requires additional prerequisites such as biocompatibility. Two excellent review articles on the topic of biochar electrodes for microbial fuel cells have been published by Yang and Chen (Yang and Chen, 2020) and by Chakraborty et al. (Chakraborty et al., 2020). In this case, the biochar may even have beneficial properties. The natural structure of plant materials can be exploited as demonstrated by Chen et al. using carbonized *Hibiscus cannabinus* as anode material for the MFC (Chen et al., 2012).

A lignocellulosic material that has not yet been adequately studied and utilized is green waste. Green waste is biogenic waste that is primarily generated in urban areas consisting mainly of grasses, leaves, and small branches. The material is usually composted or used in biogas plants, which is why the biomass is not sufficiently utilized. We have summarized the properties of green waste and possible material recycling methods in a review article (Langsdorf et al., 2021). Previously, grasses have been carbonized and investigated as electrode materials such as big bluestem for use in supercapacitors (Jin et al., 2014). Kabir et al. have demonstrated pyrolysis of real municipal green waste for the production of bio-oil, biochar, and syngas (Kabir et al., 2015). However, the production of biochar by pyrolysis from green waste as electrode material for bioelectrochemical systems has not yet been investigated. The use of carbonized green waste as electrode material in bioelectrochemical systems offers an opportunity to make the recycling of green waste more meaningful in the future. At the same time, the use of waste as electrode material can make the operation of bioelectrochemical systems more sustainable and cost-effective.

In this work, we aim to produce biochar from grass clippings as the main component of green waste for use as electrode material for bioelectrochemical systems. The production of biochar from green waste with the aim of using it as an electrode material has so far been insufficiently investigated. After carbonization, we demonstrate the production and characterization of electrodes before investigating their suitability for microbial electrosynthesis and microbial fuel cells. To the best of our knowledge, this is the first time that carbonized green waste has been used as an electrode material for bioelectrochemical systems.

2. Materials and methods

2.1. Carbonization of grass clippings

When selecting the raw material, care was taken to use a homogeneous and contamination-free starting material from one source in order to minimize any influences on the biochar characteristics. For this reason, grass clippings as the main component of green waste were used as a model substrate. The grass clippings used were sports and play turf, consisting of German pasture grass (*Lolium perenne*), regenerated with meadow grass (*Poa pratensis*). The grass clippings were harvested on the 4th of May 2020 from the VfB Zwenkau 02 e.V. sports field (Eythraer Weg 2, 04442 Zwenkau, Saxony, Germany; coordinates: 51°13'05.1"N 12°19'03.5"E) and then stored at -18 °C. To remove potential contaminants, the grass was first washed with water before being compacted for carbonization. In the first step, the grass was hydrothermally carbonized for 17 h at 250 °C and up to 55 bar pressure under a nitrogen atmosphere in an LA 500 Autoclave (VEB MLW Medizintechnik, Leipzig, Germany). The ratio of grass dry matter to process water was 1:8. After carbonization, the raw biochar was filtered from the process water, washed with water, dried to constant weight, and finally finely ground. Subsequently, the product was pyrolyzed at 850 °C for 3 to 6 min in an annealing tube furnace (ELTRA, Haan, Germany). The pyrolysis was carried out in a nitrogen countercurrent (250 L h⁻¹). After the final product had cooled down, it was finely ground again.

2.2. Manufacturing of electrodes from carbonized grass clippings

To produce the carbonized grass electrodes (CGE), a mixture of biochar and binder was applied to a metallic carrier. For this purpose, a binder solution containing 100 g L⁻¹ PVDF in DMSO was prepared. Dimensionally stable anodes (DSA, titanium expanded metal electrodes coated with iridium mixed oxide from Metakem GmbH, Usingen, Germany) were used as the metallic carrier. The DSA carrier had dimensions of 25×55 mm and thus a total geometric surface area of 27.5 cm². 1 g of biochar was mixed with 1 mL of the 10 % PVDF solution and applied to 80 % of the DSA carrier surface area (when using the electrodes, only the coated part was immersed in the electrolyte). The electrodes were dried hanging for at least two days at room temperature.

2.3. Characterization of biochar and carbonized grass electrodes

The chemical analysis of the biochar produced was carried out by elemental analysis and determination of the ash content. Elemental analysis was used to determine the total content of the elements H, C, N, and S. The measurements were carried out in tin boats with a vario MACRO cube (Elementar Analysensysteme, Langensfeld, Germany). To determine the ash content, a defined quantity of the biochar was weighed into a ceramic crucible and the sample was incinerated at 815 °C in an oxygen atmosphere. The ash content was calculated by differential weighing of the used and remaining substance. The oxygen content was determined indirectly by summing the mass percentages of the elemental analysis and the ash content.

The conductivity of the pyrolyzed biochar was determined indirectly by an electrical resistance measurement. For this purpose, 0.66 g of biochar was placed in a non-conductive hollow cylinder with an internal

diameter of 8 mm, which was sealed on both sides with a brass cylinder. The carbon layer was pressed to a defined thickness of 9.9 mm. The electrical resistance of the carbon layer was measured using a multimeter.

The mass-specific surface area of the biochar was determined at a service unit at KIT using the BET method in a gas sorption meter (Autosorb-1, Quantachrome Instruments, Boynton Beach, FL, USA) with nitrogen as adsorbate. In preparation for the BET analysis, the samples were heated at 300 °C under vacuum for at least 18 h. The BET evaluation was done in the relative pressure range of $0.02 < p/p_0 < 0.12$. The BET analysis was carried out for three samples of pyrolyzed grass biochar in multiple determinations.

Scanning electron microscope (SEM, Carl Zeiss, Oberkochen, Germany) images were taken of the biochar and the CGE produced as well as commercial graphite electrodes to assess the surface structure.

Cyclic voltammetry was performed in 0.2 M potassium phosphate buffer ($\text{KH}_2\text{PO}_4/\text{K}_2\text{HPO}_4$) including 0.1 M KCl in an electrochemical reactor (shown in Figure S1) with 100 mM $\text{K}_3[\text{Fe}(\text{CN})_6]$. For this purpose, a 3-electrode setup was employed with DSA or the CGE as the working electrode, DSA as the counter electrode, and an Ag/AgCl/ KCl_{sat} electrode (Xylem Analytics, Weilheim, Germany) as the reference electrode. The reference electrode was inserted via a Haber-Luggin capillary filled with saturated KCl. The working and counter electrodes each had a geometric surface area of 5 cm^2 ($25 \times 10 \text{ mm}$) immersed in the electrolyte. Prior to the experiments, the buffer was gassed with nitrogen for 30 min. The potential range from -0.2 V to 0.8 V vs. Ag/AgCl/ KCl_{sat} was scanned with a potentiostat (Interface 1010B, Gamry Instruments, Warminster, PA, USA) at scan rates of 2, 5, 10, and 20 mV s^{-1} starting at -0.2 V , with the third cycle being used for evaluation. The experiments were carried out as triplicates.

For linear sweep voltammetry (LSV), the same experimental setup was used as in cyclic voltammetry experiments. However, linear sweep voltammetry was carried out in the minimal medium for *Cupriavidus necator*, which is described below. In addition, the geometric surface area of the working and counter electrodes immersed in the electrolyte solution during the LSV was 15 cm^2 ($25 \times 30 \text{ mm}$) each. Linear sweep voltammetry was performed in the potential range from 0 to -2 V vs. Ag/AgCl/ KCl_{sat} at a scan rate of 20 mV s^{-1} with a potentiostat (Interface 1010B, Gamry Instruments, Warminster, PA, USA). The experiments were carried out as triplicates.

2.4. Application of carbonized grass electrodes in microbial electrosynthesis

First, the application of the CGE was investigated in microbial electrosynthesis (MES). The microorganism *Cupriavidus necator* H16 PHB⁴ (DSM-541, DSMZ, Braunschweig, Germany) was used for this purpose. By using the polyhydroxybutyrate (PHB)-deficient strain, the growth of the organism could be assessed via the optical density (OD_{600}) without being influenced by PHB production. As described above, the organism is able to grow autotrophically using H_2 , O_2 , and CO_2 . H_2 and O_2 were produced *in situ* by water electrolysis, while CO_2 was fed into the reactor. The minimal medium suitable for bioelectrochemical systems for *C. necator* was described previously (Sydow et al., 2017). The medium consisted of $2.895 \text{ g L}^{-1} \text{ Na}_2\text{HPO}_4$, $2.707 \text{ g L}^{-1} \text{ NaH}_2\text{PO}_4 \times \text{H}_2\text{O}$, $0.17 \text{ g L}^{-1} \text{ K}_2\text{SO}_4$, $0.097 \text{ g L}^{-1} \text{ CaSO}_4 \times 2 \text{ H}_2\text{O}$, $0.8 \text{ g L}^{-1} \text{ MgSO}_4 \times 7 \text{ H}_2\text{O}$, and $0.934 \text{ g L}^{-1} (\text{NH}_4)_2\text{SO}_4$ as well as trace elements: $750 \mu\text{g L}^{-1} \text{ FeSO}_4 \times 7 \text{ H}_2\text{O}$, $120 \mu\text{g L}^{-1} \text{ MnSO}_4 \times \text{H}_2\text{O}$, $120 \mu\text{g L}^{-1} \text{ ZnSO}_4 \times 7 \text{ H}_2\text{O}$, $24 \mu\text{g L}^{-1} \text{ CuSO}_4 \times 5 \text{ H}_2\text{O}$, $90 \mu\text{g L}^{-1} \text{ Na}_2\text{MoO}_4 \times 2 \text{ H}_2\text{O}$, $75 \mu\text{g L}^{-1} \text{ NiSO}_4 \times 6 \text{ H}_2\text{O}$, and $2 \mu\text{g L}^{-1} \text{ CoSO}_4 \times 7 \text{ H}_2\text{O}$.

The electrochemical reactor (shown in Figure S1) was filled with a total volume of 85 mL medium. An undivided two-electrode setup consisting of a working and counter electrode was chosen for the MES. Dimensionally stable anodes (DSA, titanium expanded metal electrodes coated with iridium mixed oxide from Metakem GmbH, Usingen, Germany) with a total geometric surface area of 27.5 cm^2 ($25 \times 55 \text{ mm}$) were

used as counter electrodes. Either the CGE or, for comparison, a DSA was used as the working electrode. A PTFE mesh was used to separate the working and counter electrodes from each other but to keep them in parallel orientation with a distance of 2 mm. A photograph of the working and counter electrode assembly is shown in the supplementary materials in Figure S2. In the experiments, the electrodes had a geometric surface area of 20 cm^2 (electrode surface area immersed in the electrolyte; $25 \times 40 \text{ mm}$) and were contacted with a titanium wire with a diameter of 0.5 mm. The reactors were stirred with a stirring bar at 200 rpm and tempered to 30 °C in an incubation hood (TH 30, Edmund Bühler GmbH, Bodelshausen, Germany). Reactors were gassed with N_2/CO_2 (80:20) at a gas flow rate of 20 mL min^{-1} . For water electrolysis, a current of -15 mA (-0.75 mA cm^{-2}) was applied via a potentiostat (Interface 1010B, Gamry Instruments, Warminster, PA, USA).

For inoculation of microbial electrosynthesis, a consecutive seed train of heterotrophic cultivation in LB medium, heterotrophic cultivation in minimal medium, and autotrophic cultivation in minimal medium is applied. The heterotrophic preculture in LB medium is inoculated from a cryo-culture of *C. necator* H16 PHB⁴. The LB medium comprised $5 \text{ g L}^{-1} \text{ NaCl}$, 5 g L^{-1} yeast extract, and 10 g L^{-1} trypticase peptone. 4 g L^{-1} fructose was added to the heterotrophic cultivation in the minimal medium as carbon source. A gas phase of $\text{H}_2/\text{O}_2/\text{CO}_2$ (64:16:20) was added to the autotrophic preculture in a septum flask at a pressure of 1.5 bar. The precultures were each inoculated from the previous preculture in late exponential to early stationary phase to an OD_{600} of 0.1 and were incubated at 30 °C and 180 rpm. With the autotrophic preculture in the late exponential to early stationary phase, the MES was inoculated to an OD_{600} of 0.2. Each day, 1 mL of sample is drawn to determine OD_{600} and pH value.

2.5. Application of carbonized grass electrodes in a microbial fuel cell

The microorganism *Geobacter sulfurreducens* (DSM-12,127, DSMZ, Braunschweig, Germany) was used to investigate the CGE in a microbial fuel cell. The medium for *G. sulfurreducens* consisted of $1.5 \text{ g L}^{-1} \text{ NH}_4\text{Cl}$, $0.6 \text{ g L}^{-1} \text{ Na}_2\text{HPO}_4$, $0.1 \text{ g L}^{-1} \text{ KCl}$, $0.82 \text{ g L}^{-1} \text{ Na-acetate}$, $2.5 \text{ g L}^{-1} \text{ NaHCO}_3$, 1 % (v/v) mineral solution, and 1 % (v/v) vitamin solution. The mineral solution contained 1.5 g L^{-1} nitrilotriacetic acid, $3 \text{ g L}^{-1} \text{ MgSO}_4 \times 7 \text{ H}_2\text{O}$, $0.5 \text{ g L}^{-1} \text{ MnSO}_4 \times \text{H}_2\text{O}$, $1 \text{ g L}^{-1} \text{ NaCl}$, $0.1 \text{ g L}^{-1} \text{ FeSO}_4 \times 7 \text{ H}_2\text{O}$, $0.18 \text{ g L}^{-1} \text{ CoSO}_4 \times 7 \text{ H}_2\text{O}$, $0.10 \text{ g L}^{-1} \text{ CaCl}_2 \times 2 \text{ H}_2\text{O}$, $0.18 \text{ g L}^{-1} \text{ ZnSO}_4 \times 7 \text{ H}_2\text{O}$, $0.01 \text{ g L}^{-1} \text{ CuSO}_4 \times 5 \text{ H}_2\text{O}$, $0.02 \text{ g L}^{-1} \text{ KAl(SO}_4)_2 \times 12 \text{ H}_2\text{O}$, $0.01 \text{ g L}^{-1} \text{ H}_3\text{BO}_3$, $0.01 \text{ g L}^{-1} \text{ Na}_2\text{MoO}_4 \times 2 \text{ H}_2\text{O}$, $0.03 \text{ g L}^{-1} \text{ NiCl}_2 \times 6 \text{ H}_2\text{O}$, $0.3 \text{ mg L}^{-1} \text{ Na}_2\text{SeO}_3 \times 5 \text{ H}_2\text{O}$, and $0.4 \text{ mg L}^{-1} \text{ Na}_2\text{WO}_4 \times 2 \text{ H}_2\text{O}$. The pH value of the mineral solution was adjusted to 7.0 with KOH. The vitamin solution contained 2 mg L^{-1} biotin, 2 mg L^{-1} folic acid, 10 mg L^{-1} pyridoxine-HCl, 5 mg L^{-1} thiamine-HCl, 5 mg L^{-1} riboflavin, 5 mg L^{-1} nicotinic acid, $5 \text{ mg L}^{-1} \text{ Ca-d-pantothenate}$, 0.1 mg L^{-1} vitamin B12, 5 mg L^{-1} p-aminobenzoic acid, and 5 mg L^{-1} (\pm)- α -lipoic acid. The whole medium had a pH value of 6.8.

The microbial fuel cell was conducted in an electrochemical H-cell (shown in Figure S3) consisting of two chambers separated by a proton exchange membrane (NafionTM 117, QuinTech, Göppingen, Germany) with a surface area of 4.9 cm^2 . The two chambers were each filled with 100 mL medium. However, mineral and vitamin solutions were only added in the anodic chamber. Either commercial cylindrical graphite rods (Graphite24, Bad Breisig, Germany) with a diameter of 15 mm or the CGE were used as both working and counter electrodes. The electrodes were contacted with a titanium wire with a diameter of 0.5 mm. The geometric electrode surface area at the start of the experiment was 15.8 and 22.5 cm^2 ($25 \times 45 \text{ mm}$) for the graphite electrodes and the CGE, respectively. An Ag/AgCl/ KCl_{sat} electrode (Xylem Analytics, Weilheim, Germany) was used as the reference electrode, which was introduced into the anode chamber by using a Haber-Luggin capillary filled with saturated KCl. The medium in the anode chamber was gassed with N_2/CO_2 (80:20) before starting the MFC. During the experiments, the medium in the anode chamber was also gassed with N_2/CO_2 (80:20) at a

gassing rate of 30 mL min⁻¹. A potential of 400 mV vs. Ag/AgCl/KCl_{sat} was applied via a potentiostat (MultiEmStat3+, PalmSens BV, Houten, Netherlands). The anode and cathode chambers were stirred with a stirrer bar at 200 rpm and the entire setup was tempered to 30 °C in an incubation hood (CERTOMAT® HK, Sartorius, Göttingen, Germany).

For the preculture, 8 g L⁻¹ Na₂-fumarate was added to the medium as electron acceptor. The preculture was cultivated from a cryo-culture of *G. sulfurreducens* in 50 mL medium with a gas phase of N₂/CO₂ (80:20) at a pressure of 1.4 bar in 250 mL septum flasks for four days at 30 °C and 180 rpm until it reached a final OD₆₀₀ of approximately 0.5. The anode chamber was inoculated with 1 mL of the preculture. To determine the acetate concentration, 1 mL of sample was taken daily and stored at -20 °C until analysis. The acetate concentration was quantified by HPLC with an Aminex HPX-87H (Bio-Rad Laboratories, Hercules, CA, USA). The mobile phase was 5 mM H₂SO₄ with a flow rate of 0.6 mL min⁻¹. The column was heated to 60 °C and detection was performed at 210 nm.

3. Results and discussion

3.1. Abiotic characterization of the carbonized grass electrodes

The biochar produced from grass clippings using hydrothermal carbonization and pyrolysis was analyzed for its elemental composition. The biochar consists of 57.4 ± 5.9 % C, 4.0 ± 0.3 % N, 3.8 ± 1.5 % O, 1.4 ± 0.1 % H, 0.4 ± 0.2 % S, and 33.1 ± 6.0 % ash (*n* = 8). In another work, a carbon content of 87.5 % was achieved for mixed green waste biochar at 750 °C with a residence time of pyrolysis of 10 min (Ronsse et al., 2013). With higher pyrolysis temperature as well as duration, the carbon content of biochar can be increased (Ronsse et al., 2013). The electrical conductivity of biochar depends on the carbon content and the structure of the carbon (graphene/graphite) (Gabhi et al., 2017). Generally, the graphite content and thus the electrical conductivity also increase with higher pyrolysis temperature (Gabhi et al., 2020). However, with increasing pyrolysis time and temperature, the yield decreases, which is why it is necessary to find a compromise. Here, the biochar shows an electrical resistance of 0.71 ± 0.33 Ω cm⁻¹ (*n* = 8). Similar values were obtained, for example, for carbonized coconut shells with 0.39 Ω cm⁻¹ (Chen et al., 2016) or carbonized kenaf stalks with 0.67 Ω cm⁻¹ (Chen et al., 2012).

The BET analysis of three grass biochar batches showed a specific surface area of 47.0 ± 4.5 m² g⁻¹ (*n* = 5), 46.2 ± 1.6 m² g⁻¹ (*n* = 3), and 51.0 ± 4.5 m² g⁻¹ (*n* = 4). Previously, biochar from green waste (slow pyrolysis at 600 °C for 60 min) showed a specific surface area of 46 m² g⁻¹ (Ronsse et al., 2013). Thus, the specific surface area of the carbonized grass clippings is in a very similar range to the biochar from mixed green waste (with different pyrolysis parameters). Chemical and thermal activation methods are described in the literature to increase the surface area of biochar (Jin et al., 2014; Dehkhoda et al., 2014; Ding et al., 2020; González-García et al., 2013). In our case, we did not use chemical activation with KOH, as it did not increase the final carbon content (data not shown). However, this could improve the properties of the biochar, depending on the field of application. Furthermore, the specific surface area of biochar also generally increases with higher pyrolysis temperatures (Ronsse et al., 2013).

We tested various methods for the production of electrodes from the carbonized grass clippings. We attempted to press electrodes from the biochar with and without binders and also without the use of a metallic carrier/electrode support. Compacting the biochar can further increase the electrical conductivity (Adinaveen et al., 2016). While the remaining lignin in biochar from hydrothermal carbonization serves as a binder when the biochar is pressed (Reza et al., 2012), pressing the biochar after pyrolysis without additional binder did not result in mechanically stable pellets in our case. Additionally, without a metallic carrier, electrically contacting the pressed electrodes was inconvenient. A proven method of fabricating electrodes from biochar is to apply the biochar to a metallic current collector using a binder such as PVDF or

PTFE (Jin et al., 2014; Ding et al., 2020), which is why we chose that method. Fig. 1 shows one of the electrodes produced. The electrodes can be designed to be recyclable if a sustainable binder is used and by eliminating the metallic carrier. By additive manufacturing, electrodes with variable geometries can be created from the biochar (Idrees et al., 2018). To improve mass transfer in a bioelectrochemical system, the biochar could also be granulated (Ren et al., 2015) and used as a granular electrode in a fluidized bed reactor (Dong et al., 2018). More robust biochar electrode manufacturing processes suitable for mass production, such as screen printing, remain to be investigated.

The biochar and the CGE were examined in comparison to a commercial graphite electrode under the SEM regarding surface structure (Fig. 2). The graphite electrode shows a rough surface structure (a), while the biochar has clearer pores (b). The surface of the finished CGE is considerably coarser (c), which could promote biofilm formation. At a higher magnification, the polymer structure of the PVDF binder is clearly recognizable (d).

Fig. 3 shows the cyclic voltammograms of the redox probe K₃Fe(CN)₆ with a DSA as the working electrode (a) compared to a CGE as the working electrode (b). While the typical redox peaks can be measured in the cyclic voltammogram with the DSA, the peaks are less pronounced when using the CGE. The current at the lower and upper potentials might be attributed to unspecified side reactions or the pattern of an ohmic resistance. Nevertheless, it can be stated that both oxidation of Fe²⁺ and reduction of Fe³⁺ are detectable at the fabricated electrodes. In a linear sweep experiment in the medium for the MES (Figure S4), an earlier and greater current response with increasing potential can be observed using the CGE compared to the DSA, which might be mainly attributed to a higher electrode resistance and an ohmic behavior. With both electrodes, visible bubble formation on the working electrode indicating hydrogen evolution can only be seen from around -700 to -800 mV in all experiments.

3.2. Application of carbonized grass electrodes in microbial electrosynthesis

First, the carbonized grass electrodes were investigated for use in microbial electrosynthesis. For this purpose, *Cupriavidus necator* PHB⁻4 was cultivated electroautotrophically at a constant current density of -0.75 mA cm⁻² over seven days. The CGE was compared with a DSA as

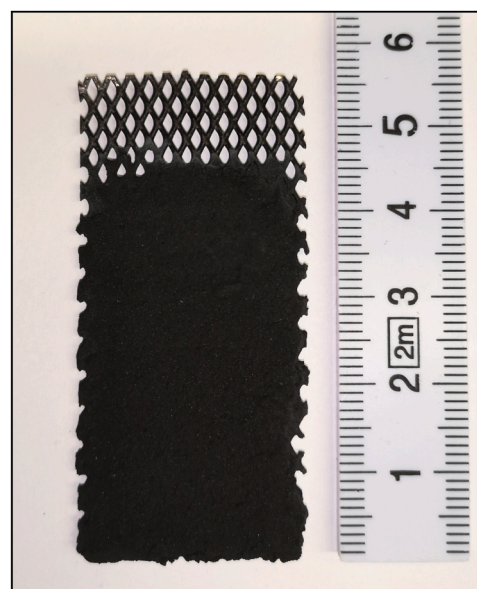


Fig. 1. Manufactured carbonized grass electrode: 1 g of biochar mixed with 1 mL of the 10 % PVDF solution in DMSO applied to 80 % of the DSA metal carrier with dimensions of 25×55 mm.

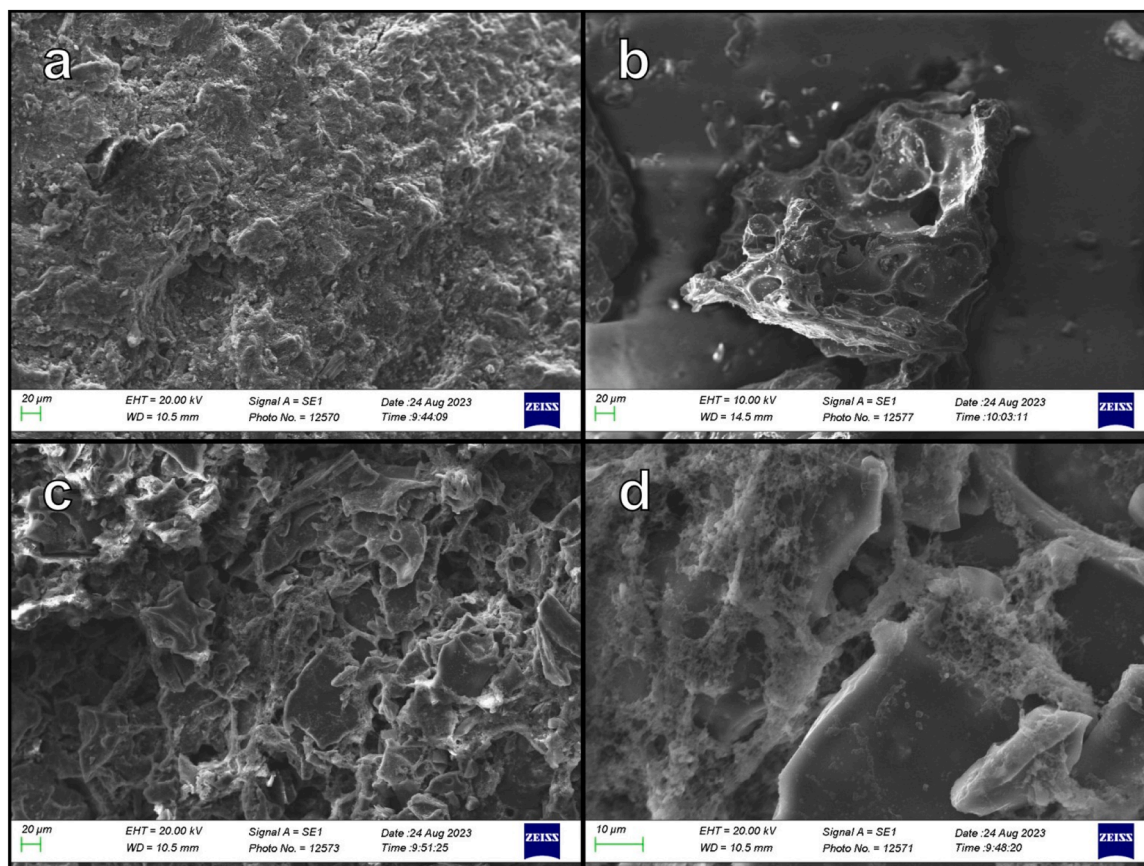


Fig. 2. SEM images of a commercial graphite rod (a), a grass biochar particle (b), and a carbonized grass electrode at lower (c) and higher magnification (d).

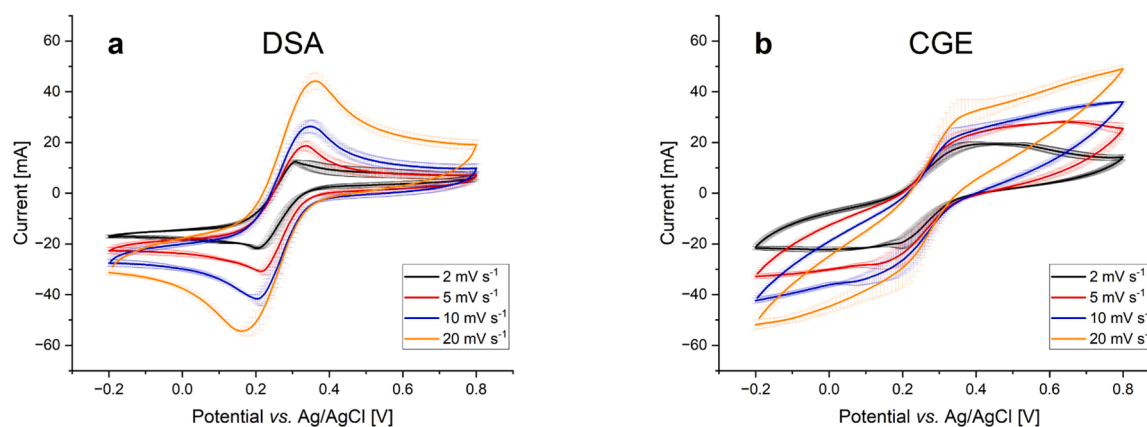


Fig. 3. Cyclic voltammetry of 100 mM $K_3Fe(CN)_6$ with DSA (a) or carbonized grass electrode (CGE) (b) as working electrode at scan rates of 2, 5, 10, and 20 $mV s^{-1}$ ($n = 3$). DSA as counter electrode each, geometric surface area of both working and counter electrode of 5 cm^2 , Ag/AgCl/ KCl_{sat} reference electrode, and 0.2 M potassium phosphate buffer with 0.1 M KCl as electrolyte.

the working electrode for the hydrogen evolution reaction. Fig. 4 shows the course of OD_{600} (a) as well as pH value and potential vs. Ag/AgCl/ KCl_{sat} (b) of the two experiments. Faster microbial growth can be observed when the DSA is used as a working electrode. While an average OD_{600} of 1.7 ± 0.4 is achieved with the DSA after seven days, the use of the CGE only results in an OD_{600} of 1.1 ± 0.3 . Differences can also be seen in the pH value and potential curves. The pH value of the DSA experiment drops from 6.6 ± 0.0 to 6.2 ± 0.1 during the experiment. When using the CGE, the pH value drops from 6.6 ± 0.1 to 5.5 ± 0.2 . Since the organism in the experiment with the CGE shows lower growth, it is unlikely that the pH value drop has a biological origin but rather an

electrochemical one. However, the pH value is still in a range in which it should not have a notable influence on the growth of the microorganism. The potential curve is relatively linear during both experiments, although it is about 0.35 V more negative for the CGE. The higher potential indicates either a higher electrode resistance or a higher overpotential for the desired hydrogen evolution reaction at the CGE. During the linear sweep experiment (Figure S4), a higher current response with increasing potential and a current response before the actual water electrolysis can be seen with the CGE compared to the DSA. The results are reflected in the electrical potential during the MES. It was not to be expected that the CGE would outperform the DSA, as the DSA is

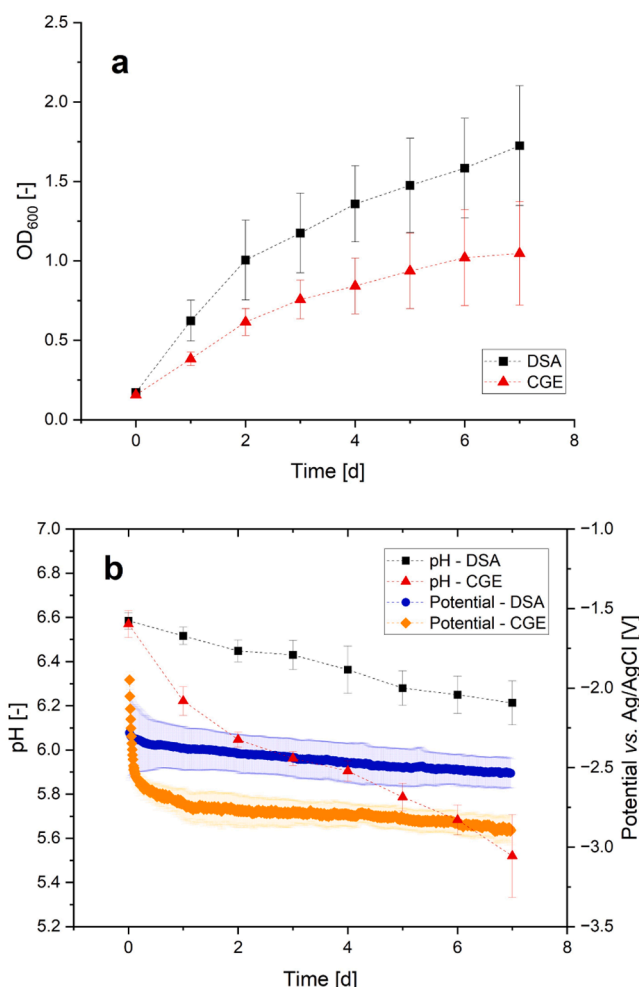


Fig. 4. Course of OD₆₀₀ (a) as well as pH value and potential vs. Ag/AgCl/KCl_{sat} (b) during electroautotrophic cultivation of *Cupriavidus necator* PHB[−]4 with a DSA and a carbonized grass electrode (CGE) as working electrode ($n = 3$). Temperature of 30 °C, mixing at 200 rpm, minimal medium with an initial volume of 85 mL, gassing rate of 20 mL min^{−1} with N₂/CO₂ (80:20), constant current density of -0.75 mA cm^{−2} for water electrolysis, DSA as counter electrode each, geometric surface area of both working and counter electrode of 20 cm², and Ag/AgCl/KCl_{sat} reference electrode. Dashed lines serve as a guide to the eye.

optimized for the oxygen evolution reaction in water electrolysis and has a lower resistance. The lignocellulosic biochar also cannot compete with specialized carbon-based electrodes, such as customized carbon nanotubes or nanorods designed specifically for the hydrogen/oxygen evolution reaction (Liu et al., 2024; You et al., 2023; Deng et al., 2023) or battery solutions (Zhong et al., 2023; Zhang et al., 2022). However, the electrochemical performance of the CGE could be optimized by adapting the carbonization process, by chemical pretreatment prior to carbonization or by incorporating conductive material into the CGE during manufacture.

3.3. Application of carbonized grass electrodes in a microbial fuel cell

After the application in microbial electrosynthesis, the carbonized grass electrodes were investigated for use in microbial fuel cells. For this purpose, a microbial fuel cell with *Geobacter sulfurreducens* was conducted either with graphite electrodes (GE) or the CGE. Fig. 5a shows the current density and the acetate concentration throughout the two experiments. Compared to the graphite electrodes, an earlier current response can be seen in the experiment with the CGE. As a result, acetate

can no longer be detected one day earlier. One reason for this could be faster biofilm formation due to more advantageous surface properties. The coarser surface structure was confirmed with the SEM (see above). Since different precultures were used for the triplicates, the influence of the preculture on the current response can be excluded. The absolute current response is higher with the graphite electrodes. The integral of the current curve results in an electric charge of 39.4 ± 1.9 and 25.1 ± 4.1 As cm^{−2} for the graphite electrodes and CGE, respectively. This could be due to the higher conductivity of the graphite electrodes, benefiting electron transfer. Nevertheless, we were able to show that the electrodes from carbonized grass clippings are suitable for microbial fuel cells and may have advantageous properties.

In a subsequent experiment, we investigated whether the electrodes are also suitable over a longer period of time. For this purpose, three microbial fuel cells were set up with the CGE as before. The current response was recorded over several weeks. 20 mM acetate was added when the current dropped. Fig. 5b shows the current density curve of the three MFCs. Cells A and C ran successfully for 44 and 45 days, respectively. Due to technical difficulties with cell B, which were unrelated to the CGE, the experiment had to be aborted after 25 days. No restrictions due to the electrodes were observed throughout the experiment. The experiment could likely have run for much longer, indicating a stable electrode performance. Commault et al. demonstrated an MFC with (modified) graphite rods as electrodes and a *Geobacter*-dominated biofilm using acetate/ethanol medium and synthetic wastewater that was active for 75 days (Commault et al., 2015). Throughout the experiment shown, varying current responses were observed, particularly in cell C, which could be due to varying substrate concentrations. In addition, adaptation effects of the microorganism could already occur over the duration of the experiment. Differences in the biofilm may also be a reason, as only the living cells are responsible for the electrochemical activity (D. Sun et al., 2016).

The results of the MFC have shown that electrodes made from carbonized grass clippings can certainly be an alternative to fossil graphite. However, different challenges could arise when using residual materials. One challenge could be possible contamination by e.g., plastic in the raw material. Furthermore, it remains to be investigated what influence the heterogeneity of the starting material due to seasonality has on the result of the carbonization. Another major obstacle to the use of pyrolyzed waste materials as electrode material is the high energy input required for carbonization. Electrode fabrication seems to be a promising method in colder seasons because there is less liquid in the green waste during that time. In addition, much of the green waste in winter is foliage, which contains little lignin and thus allows for easier carbonization. To further increase the efficiency of pyrolysis, the solid part could be separated from the liquid part of the green waste beforehand, for example by pressing. Then only the solid part could be pyrolyzed, while the liquid part is recycled elsewhere. Previously, we have shown that the juice from grass clippings can serve as a growth medium for *C. necator* (Langsdorf et al., 2022). The combination of biorefineries for the use of biogenic feedstocks and bioelectrochemical transformations for coupling electrical energy with the chemical industry offers huge potential for a future bio-based economy (Harnisch and Urban, 2018).

4. Conclusions

For the first time, we demonstrated the manufacturing of electrodes from carbonized grass clippings and their application in bioelectrochemical systems. The greatest potential of biochar electrodes lies in technologies that use graphite or similar materials as electrodes. We were able to show that electrodes from carbonized grass clippings perform similarly to commercial graphite electrodes in the microbial fuel cell and that they can be used for more than six weeks, probably even much longer. This work once again shows the potential of renewable raw materials as a starting material for electrodes as well as another

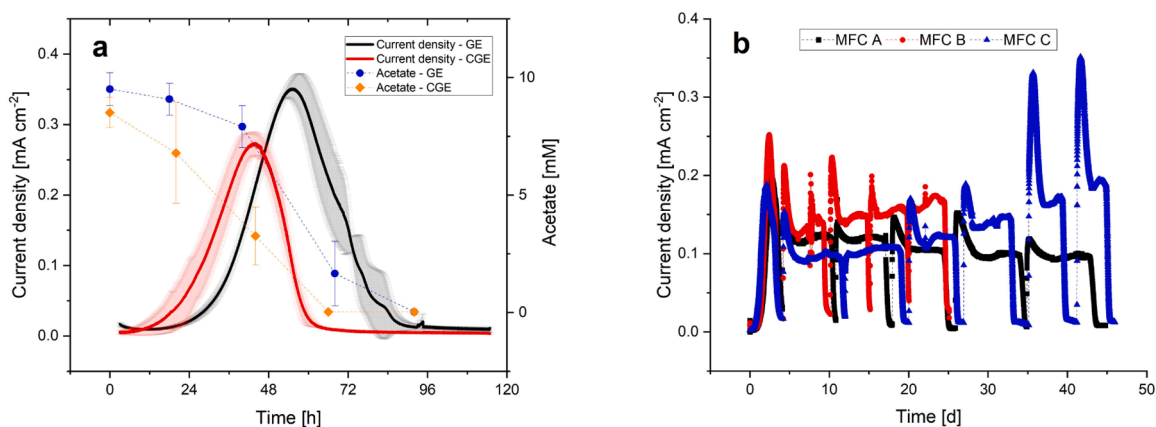


Fig. 5. Current density and acetate concentration of the MFC with *G. sulfurreducens* with graphite electrodes (GE) and carbonized grass electrodes (CGE) each as working and counter electrode (a, $n = 3$) and current density of three MFC experiments titled A, B, and C with carbonized grass electrodes (b, $n = 1$). Temperature of 30 °C, mixing at 200 rpm, initial medium volume of 100 mL in anode and cathode chamber, separation of the anode and cathode chambers by a proton exchange membrane (Nafion™ 117) with a surface area of 4.9 cm², gassing rate of 30 mL min⁻¹ with N₂/CO₂ (80:20), constant potential of 400 mV vs. Ag/AgCl/KCl_{sat}, geometric surface area of GE and CGE of 15.8 and 22.5 cm² respectively, and Ag/AgCl/KCl_{sat} reference electrode. Dashed lines serve as a guide to the eye.

method of recycling green waste material.

CRediT authorship contribution statement

Alexander Langsdorf: Conceptualization, Methodology, Investigation, Writing – original draft, Visualization. **Michael Halim:** Methodology, Investigation, Writing – review & editing. **Marianne Volkmar:** Conceptualization, Writing – review & editing. **Markus Stöckl:** Conceptualization, Writing – review & editing. **Ralf Harnisch:** Investigation, Writing – review & editing. **Peter Hahn:** Conceptualization, Methodology, Writing – review & editing, Supervision. **Roland Ulber:** Conceptualization, Writing – review & editing, Funding acquisition. **Dirk Holtmann:** Conceptualization, Methodology, Writing – review & editing, Project administration, Funding acquisition.

Declaration of competing interest

The authors declare that they have no known competing financial interests or personal relationships that could have appeared to influence the work reported in this paper.

Data availability

Data will be made available on request.

Funding

This research was prepared within the project “Green-ToGreen—municipal green waste as a basis for green chemistry” from the innovation space “BioBall”, which was funded by the German Federal Ministry of Education and Research (BMBF, grant numbers: 031B0903A, 031B0903B, and 031B0903C).

Acknowledgements

We would like to thank Tim Nicklas Crienitz and Julian Philipp Schütz for their outstanding commitment during their bachelor thesis. In addition, we would like to thank Elke Landrock-Bill for the scanning electron microscope images as well as Klaus Hirsch and the Particle Measurement Technology group at the Institute of Mechanical Process Engineering and Mechanics of the Karlsruhe Institute of Technology for the BET analysis.

Supplementary materials

Supplementary material associated with this article can be found, in the online version, at [doi:10.1016/j.clee.2024.100118](https://doi.org/10.1016/j.clee.2024.100118).

References

- Adinaveen, T., Vijaya, J.J., Kennedy, L.J., 2016. Comparative study of electrical conductivity on activated carbons prepared from various cellulose materials. *Arab. J. Sci. Eng.* 41, 55–65. <https://doi.org/10.1007/s13369-014-1516-6>.
- Bond, D.R., Lovley, D.R., 2003. Electricity production by *Geobacter sulfurreducens* attached to electrodes. *Appl. Environ. Microbiol.* 69, 1548–1555. <https://doi.org/10.1128/AEM.69.3.1548-1555.2003>.
- Cancelliere, R., Carbone, K., Pagano, M., Cacciotti, I., Micheli, L., 2019. Biochar from Brewers' Spent Grain: a green and low-cost smart material to modify screen-printed electrodes. *Biosensors (Basel)* 9. <https://doi.org/10.3390/bios9040139>.
- Chakraborty, I., Sathe, S.M., Dubey, B.K., Ghangrekar, M.M., 2020. Waste-derived biochar: applications and future perspective in microbial fuel cells. *Bioresour. Technol.* 312, 123587. <https://doi.org/10.1016/j.biortech.2020.123587>.
- Chen, S., He, G., Hu, X., Xie, M., Wang, S., Zeng, D., Hou, H., Schröder, U., 2012. A three-dimensionally ordered macroporous carbon derived from a natural resource as anode for microbial bioelectrochemical systems. *ChemSusChem* 5, 1059–1063. <https://doi.org/10.1002/cssc.201100783>.
- Chen, S., Tang, J., Fu, L., Yuan, Y., Zhou, S., 2016. Biochar improves sediment microbial fuel cell performance in low conductivity freshwater sediment. *J. Soils. Sediments* 16, 2326–2334. <https://doi.org/10.1007/s11368-016-1452-z>.
- Commault, A.S., Lear, G., Weld, R.J., 2015. Maintenance of *Geobacter*-dominated biofilms in microbial fuel cells treating synthetic wastewater. *Bioelectrochemistry* 106, 150–158. <https://doi.org/10.1016/j.bioelechem.2015.04.011>.
- Dehkoda, A.M., Ellis, N., Gyenge, E., 2014. Electrosorption on activated biochar: effect of thermo-chemical activation treatment on the electric double layer capacitance. *J. Appl. Electrochem.* 44, 141–157. <https://doi.org/10.1007/s10800-013-0616-4>.
- Deng, K., Liu, P., Liu, X., Li, H., Tian, W., Ji, J., 2023. Synergism of CoO–Ni(OH) 2 nanosheets and MOF-derived CNTs array for methanol electrolysis. *Green. Chem.* 25, 9837–9846. <https://doi.org/10.1039/D3GC03179A>.
- Ding, Y., Wang, T., Dong, D., Zhang, Y., 2020. Using biochar and coal as the electrode material for supercapacitor applications. *Front. Energy Res.* 7, 159. <https://doi.org/10.3389/fenrg.2019.00159>.
- Dong, Z., Wang, H., Tian, S., Yang, Y., Yuan, H., Huang, Q., Song, T.-S., Xie, J., 2018. Fluidized granular activated carbon electrode for efficient microbial electrosynthesis of acetate from carbon dioxide. *Bioresour. Technol.* 269, 203–209. <https://doi.org/10.1016/j.biortech.2018.08.103>.
- Ferreira, P.A., Backes, R., Martins, C.A., de Carvalho, C.T., da Silva, R.A.B., 2018. Biochar: a low-cost electrode modifier for electrocatalytic, sensitive and selective detection of similar organic compounds. *Electroanalysis* 30, 2233–2236. <https://doi.org/10.1002/elan.201800430>.
- Fruehauf, H.M., Enzmann, F., Harnisch, F., Ulber, R., Holtmann, D., 2020. Microbial electrosynthesis—an inventory on technology readiness level and performance of different process variants. *Biotechnol. J.* 15, e2000066. <https://doi.org/10.1002/biot.202000066>.
- Gabhi, R.S., Kirk, D.W., Jia, C.Q., 2017. Preliminary investigation of electrical conductivity of monolithic biochar. *Carbon* N. Y. 116, 435–442. <https://doi.org/10.1016/j.carbon.2017.01.069>.

- Gabhi, R., Basile, L., Kirk, D.W., Giorcelli, M., Tagliaferro, A., Jia, C.Q., 2020. Electrical conductivity of wood biochar monoliths and its dependence on pyrolysis temperature. *Biochar*. 2, 369–378. <https://doi.org/10.1007/s42773-020-00056-0>.
- Gizewski, J., Sande, L.V.D., Holtmann, D., 2023. Contribution of electrobiotechnology to sustainable development goals. *Trends Biotechnol.* <https://doi.org/10.1016/j.tibtech.2023.02.009>.
- González-García, P., Centeno, T.A., Urones-Garrote, E., Ávila-Brandé, D., Otero-Díaz, L.C., 2013. Microstructure and surface properties of lignocellulosic-based activated carbons. *Appl. Surf. Sci.* 265, 731–737. <https://doi.org/10.1016/j.apsusc.2012.11.092>.
- Harnisch, F., Urban, C., 2018. Electrobiorefineries: unlocking the synergy of electrochemical and microbial conversions. *Angewandte Chemie Int. Edit.* 57, 10016–10023. <https://doi.org/10.1002/anie.201711727>.
- Hoffmann, V., Jung, D., Zimmermann, J., Correa, C., Rodríguez, Elleuch, A., Halouani, K., Kruse, A., 2019a. Conductive carbon materials from the hydrothermal carbonization of vineyard residues for the application in electrochemical double-layer capacitors (EDLCs) and direct carbon fuel cells (DCFCs). *Materials*. (Basel) 12. <https://doi.org/10.3390/ma12101703>.
- Hoffmann, V., Correa, C., Rodríguez, Sautter, D., Maringolo, E., Kruse, A., 2019b. Study of the electrical conductivity of biobased carbonaceous powder materials under moderate pressure for the application as electrode materials in energy storage technologies. *GCB Bioenergy* 11, 230–248. <https://doi.org/10.1111/gcbb.12545>.
- Idrees, M., Jeelani, S., Rangari, V., 2018. Three-dimensional-printed sustainable biochar-recycled PET composites. *ACS Sustain. Chem. Eng.* 6, 13940–13948. <https://doi.org/10.1021/acssuschemeng.8b02283>.
- Jara, A.D., Betemariam, A., Woldetinsae, G., Kim, J.Y., 2019. Purification, application and current market trend of natural graphite: a review. *Int. J. Min. Sci. Technol.* 29, 671–689. <https://doi.org/10.1016/j.ijmst.2019.04.003>.
- Jin, H., Wang, X., Gu, Z., Hoefelmeyer, J.D., Muthukumarappan, K., Julson, J., 2014. Graphitized activated carbon based on big bluestem as an electrode for supercapacitors. *RSC. Adv.* 4, 14136. <https://doi.org/10.1039/c3ra46037a>.
- Kabir, M., Chowdhury, A., Rasul, M., 2015. Pyrolysis of municipal green waste: a modelling, simulation and experimental analysis. *Energies*. (Basel) 8, 7522–7541. <https://doi.org/10.3390/en8087522>.
- Krieg, T., Sydow, A., Schröder, U., Schrader, J., Holtmann, D., 2014. Reactor concepts for bioelectrochemical syntheses and energy conversion. *Trends Biotechnol.* 32, 645–655. <https://doi.org/10.1016/j.tibtech.2014.10.004>.
- Krieg, T., Sydow, A., Faust, S., Huth, I., Holtmann, D., 2018. CO₂ to terpenes: autotrophic and electroautotrophic α -humulene production with *Cupriavidus necator*. *Angew. Chem. Int. Ed Engl.* 57, 1879–1882. <https://doi.org/10.1002/anie.201711302>.
- Langsdorf, A., Volkmar, M., Holtmann, D., Ulber, R., 2021. Material utilization of green waste: a review on potential valorization methods. *Bioresour. Bioprocess.* 8 <https://doi.org/10.1186/s40643-021-00367-5>.
- Langsdorf, A., Drommershausen, A.-L., Volkmar, M., Ulber, R., Holtmann, D., 2022. Fermentative α -Humulene production from homogenized grass clippings as a growth medium. *Molecules*. 27. <https://doi.org/10.3390/molecules27248684>.
- Li, Y., Zhang, X., Deng, J., Yang, X., Wang, J., Wang, Y., 2020. Hierarchical porous biochar derived from *cotinus coggygia* flower by using a novel composite activator for supercapacitors. *Chem. Phys. Lett.* 747, 137325 <https://doi.org/10.1016/j.cplett.2020.137325>.
- Liu, X., Deng, K., Liu, P., Lv, X., Tian, W., Ma, K., Li, H., Ji, J., 2024. Mutual promotion by structural design and intrinsic activity coupling of CNTs/MoC/CoNiMo for water splitting and urea electrolysis. *Appl. Catal. B: Environ.* 343, 123470 <https://doi.org/10.1016/j.apcatb.2023.123470>.
- Logan, B.E., Rossi, R., Ragab, A., Saikaly, P.E., 2019. Electroactive microorganisms in bioelectrochemical systems. *Nat. Rev. Microbiol.* 17, 307–319. <https://doi.org/10.1038/s41579-019-0173-x>.
- Purkait, T., Singh, G., Singh, M., Kumar, D., Dey, R.S., 2017. Large area few-layer graphene with scalable preparation from waste biomass for high-performance supercapacitor. *Sci. Rep.* 7, 15239. <https://doi.org/10.1038/s41598-017-15463-w>.
- Qiu, Z., Wang, Y., Bi, X., Zhou, T., Zhou, J., Zhao, J., Miao, Z., Yi, W., Fu, P., Zhuo, S., 2018. Biochar-based carbons with hierarchical micro-meso-macro porosity for high rate and long cycle life supercapacitors. *J. Power Sources* 376, 82–90. <https://doi.org/10.1016/j.jpowsour.2017.11.077>.
- Reguera, G., McCarthy, K.D., Mehta, T., Nicoll, J.S., Tuominen, M.T., Lovley, D.R., 2005. Extracellular electron transfer via microbial nanowires. *Nature* 435, 1098–1101. <https://doi.org/10.1038/nature03661>.
- Reguera, G., Pollina, R.B., Nicoll, J.S., Lovley, D.R., 2007. Possible nonconductive role of *Geobacter sulfurreducens* pilus nanowires in biofilm formation. *J. Bacteriol.* 189, 2125–2127. <https://doi.org/10.1128/JB.01284-06>.
- Ren, J., Li, N., Li, L., An, J.-K., Zhao, L., Ren, N.-Q., 2015. Granulation and ferric oxides loading enable biochar derived from cotton stalk to remove phosphate from water. *Bioresour. Technol.* 178, 119–125. <https://doi.org/10.1016/j.biortech.2014.09.071>.
- Reza, M.T., Lynam, J.G., Vasquez, V.R., Coronella, C.J., 2012. Pelletization of biochar from hydrothermally carbonized wood. *Environ. Prog. Sustain. Energy* 31, 225–234. <https://doi.org/10.1002/ep.11615>.
- Ronsse, F., van Hecke, S., Dickinson, D., Prins, W., 2013. Production and characterization of slow pyrolysis biochar: influence of feedstock type and pyrolysis conditions. *GCB Bioenergy* 5, 104–115. <https://doi.org/10.1111/gcbb.12018>.
- Stöckl, M., Teubner, N.C., Holtmann, D., Mangold, K.-M., Sand, W., 2019. Extracellular polymeric substances from *Geobacter sulfurreducens* biofilms in microbial fuel cells. *ACS Appl. Mater. Interfaces* 11, 8961–8968. <https://doi.org/10.1021/acsami.8b14340>.
- Stöckl, M., Gemünde, A., Holtmann, D., 2023. Microbial electrotechnology – intensification of bioprocesses through the combination of electrochemistry and biotechnology. *Phys. Sci. Rev.* <https://doi.org/10.1515/psr-2022-0108>, 0.
- Sun, G., Rodrigues, D.d.S., Thygesen, A., Daniel, G., Fernando, D., Meyer, A.S., 2016a. Inocula selection in microbial fuel cells based on anodic biofilm abundance of *Geobacter sulfurreducens*. *Chin. J. Chem. Eng.* 24, 379–387. <https://doi.org/10.1016/j.cjche.2015.11.002>.
- Sun, D., Chen, J., Huang, H., Liu, W., Ye, Y., Cheng, S., 2016b. The effect of biofilm thickness on electrochemical activity of *Geobacter sulfurreducens*. *Int. J. Hydrogen Energy* 41, 16523–16528. <https://doi.org/10.1016/j.ijhydene.2016.04.163>.
- Sydow, A., Krieg, T., Ulber, R., Holtmann, D., 2017. Growth medium and electrolyte-How to combine the different requirements on the reaction solution in bioelectrochemical systems using *Cupriavidus necator*. *Eng. Life Sci.* 17, 781–791. <https://doi.org/10.1002/elsc.201600252>.
- Teetz, N., Holtmann, D., Harnisch, F., Stöckl, M., 2022. Upgrading Kolbe electrolysis-highly efficient production of green fuels and solvents by coupling biosynthesis and electrosynthesis. *Angew. Chem. Int. Ed Engl.* 61, e202210596 <https://doi.org/10.1002/anie.202210596>.
- Yang, W., Chen, S., 2020. Biomass-derived carbon for electrode fabrication in microbial fuel cells: a review. *Ind. Eng. Chem. Res.* 59, 6391–6404. <https://doi.org/10.1021/acs.iecr.0c00041>.
- You, T., Deng, K., Liu, P., Lv, X., Tian, W., Li, H., Ji, J., 2023. Synergism of NiFe layered double hydroxides/phosphides and Co-NC nanorods array for efficient electrocatalytic water splitting. *Chem. Eng. J.* 470, 144348 <https://doi.org/10.1016/j.cej.2023.144348>.
- Zhan, Y., Zhou, H., Guo, F., Tian, B., Shilin, Du, Dong, Y., Qian, L., 2021. Preparation of highly porous activated carbons from peanut shells as low-cost electrode materials for supercapacitors. *J. Energy Storage* 34, 102180. <https://doi.org/10.1016/j.est.2020.102180>.
- Zhang, L., Jiang, J., Holm, N., Chen, F., 2014. Mini-chunk biochar supercapacitors. *J. Appl. Electrochem.* 44, 1145–1151. <https://doi.org/10.1007/s10800-014-0726-7>.
- Zhang, B., Jiang, Y., Balasubramanian, R., 2021. Synthesis, formation mechanisms and applications of biomass-derived carbonaceous materials: a critical review. *J. Mater. Chem. A* 9, 24759–24802. <https://doi.org/10.1039/D1TA06874A>.
- Zhang, T., Liu, P., Zhong, Y., Zheng, J., Deng, K., Lv, X., Li, H., Tian, W., Ji, J., 2022. N, S co-doped branched carbon nanotubes with hierarchical porous structure and electron/ion transfer pathways for supercapacitors and lithium-ion batteries. *Carbon*. N. Y. 198, 91–100. <https://doi.org/10.1016/j.carbon.2022.07.015>.
- Zhong, Y., Deng, K., Zheng, J., Zhang, T., Liu, P., Lv, X., Tian, W., Ji, J., 2023. One-step growth of the interconnected carbon nanotubes/graphene hybrids from cuttlebone-derived bi-functional catalyst for lithium-ion batteries. *J. Mater. Sci. Technol.* 149, 205–213. <https://doi.org/10.1016/j.jmst.2022.11.035>.
- Zhu, H., Wang, X., Yang, F., Yang, X., 2011. Promising carbons for supercapacitors derived from fungi. *Adv. Mater.* 23, 2745–2748. <https://doi.org/10.1002/adma.201100901>.